The synthesis of oxyhalogen complexes of substitution inert metal ions remains a difficult task. Chloratopentaaquo-chromium(III) and chloritopentaamminecobalt(III) have been prepared, but by admittedly fortuitous pathways in appropriate oxidation–reduction reactions. The iodate salt of iodato-pentaamminechromium(III) has been isolated but rapidly forms the aquo complex in solution via breakage of the iodine(V)–oxygen bond.[25] Modifications of the synthesis described herein may allow the preparation of chlorito complexes of metal ions other than pentaamminecobalt(III). The chemistry of these complexes seems sufficiently interesting to merit further experimental effort.

Acknowledgment. We are grateful to Professor R. Kent Murmann for the preparation and mass spectrometric analysis of the CO_2 samples.

Registry No. [(NH3)5CoOClO](NO3)2, 56335-61-6; Co^{3+}, 22541-63-5; $HClO_2$, 13898-47-0; Cr^{2+}, 22541-79-3; Fe^{2+}, 15438-31-0; VO^{2+}, 20644-97-7; HSO_3^-, 15181-46-1; $(NH_3)_5CoOH_2^{3+}$, 14403-82-8.

References and Notes

(1) R. C. Thompson, *Inorg. Chem.*, **14**, 1279 (1975).
(2) R. C. Thompson and G. Gordon, *Inorg. Chem.*, **5**, 557, 562 (1966).
(3) J. C. Sullivan and R. C. Thompson, *Inorg. Chem.*, **6**, 1795 (1967).
(4) R. C. Thompson, *J. Phys. Chem.*, **72**, 2642 (1968).
(5) R. G. Keiffer and G. Gordon, *Inorg. Chem.*, **7**, 235 (1968).
(6) R. E. Kitson, *Anal. Chem.*, **22**, 664 (1950).
(7) This technique is rather sensitive. We have been able to separate solutions containing 85% $(NH_3)_5CrNO^{2+}$ and 15% $(NH_3)_4(H_2O)CrNO^{2+}$ into distinct bands.
(8) G. W. Haupt, *J. Res. Natl. Bur. Stand.*, **48**, 414 (1952).
(9) J. C. Sullivan and J. E. French, *Inorg. Chem.*, **3**, 832 (1964).
(10) (a) R. K. Murmann, *Inorg. Chim. Acta*, **25**, L43 (1977); (b) J. Halperin and H. Taube, *J. Am. Chem. Soc.*, **74**, 375 (1952).
(11) H. Goff and R. K. Murmann, *J. Am. Chem. Soc.*, **93**, 6058 (1971).
(12) B. D. Holt, *Anal. Chem.*, **49**, 1664 (1977).
(13) Two examples of weakly associated, labile complexes of chlorite ion have been reported: (a) $(UO_2 \cdot ClO_2)^+$, G. Gordon and D. M. H. Kern, *Inorg. Chem.*, **3**, 1055 (1964); (b) $(ClO_2 \cdot ClO_2)^-$, G. Gordon and F. Emmenegger, *Inorg. Nucl. Chem. Lett.*, **2**, 395 (1966).
(14) D. L. Toppen and R. G. Linck, *Inorg. Chem.*, **10**, 2635 (1971).
(15) F. Basolo and R. G. Pearson, "Mechanisms of Inorganic Reactions", 2nd ed., Wiley, New York, 1968, Chapter 3.
(16) (a) S. C. Chan and F. Leh, *J. Chem. Soc. A*, 126 (1966); (b) W. F. Richardson, Masters Thesis, University of Missouri, 1975.
(17) It has not escaped our attention that an estimate of the potential for the $(NH_3)_5Co^{3+}$, $(NH_3)_5Co^{2+}$ couple can be made by use of the free energy of activation for the decomposition of $(NH_3)_5CoOClO^{2+}$ and the standard electrode potential for the ClO_2, ClO_2^- couple, provided several speculative assumptions are made. However, this point is far removed from the thrust of the present investigation.
(18) (a) J. C. Sullivan and R. C. Thompson, *Inorg. Chem.*, **6**, 1795 (1967); (b) T. W. Newton and M. J. Burkhardt, *ibid.*, **10**, 2323 (1971).
(19) G. Davies and B. Warnqvist, *Coord. Chem. Rev.*, **5**, 349 (1970).
(20) With a large excess of cobalt(III), $d[ClO_2]/dt = k_1[comp]/(k_1 - k_2)[k_1 \exp(-k_1 t) + k_2 \exp(-k_2 t)]$ where $k_1 = [Co(III)]_0$(rate constant for comp–Co^{III}) and $k_2 = [Co(III)]_0$(rate constant for ClO_2–Co^{III}).
(21) T. C. Hoering, F. T. Ishimori, and H. O. McDonald, *J. Am. Chem. Soc.*, **80**, 3876 (1958).
(22) R. K. Murmann and R. C. Thompson, *J. Inorg. Nucl. Chem.*, **32**, 1404 (1970).
(23) (a) H. R. Hunt and H. Taube, *J. Am. Chem. Soc.*, **80**, 2642 (1958); (b) A. C. Rutenberg and H. Taube, *J. Chem. Phys.*, **20**, 825 (1952).
(24) (a) E. J. Hinderberger, Jr., and R. C. Thompson, *Inorg. Chem.*, **14**, 784 (1975); (b) C. Lavallee and T. W. Newton, *Inorg. Chem.*, **11**, 2616 (1972).
(25) T. Ramasami, R. K. Wharton, and A. G. Sykes, *Inorg. Chem.*, **14**, 359 (1975).

Chemical Reactivity of Ruthenium Complexes Supported on Y-Type Zeolites

C. P. MADHUSUDHAN, M. D. PATIL, and M. L. GOOD*

The detailed chemical reactivity of the $[Ru^{II}(NH_3)_5N_2]^{2+}$ ion supported on a Y-type zeolite has been probed by infrared and UV–visible spectroscopy. The air oxidation of the supported ruthenium complex produces a wine red species previously thought to be $[Ru^{III}(NH_3)_5OH]^{2+}$–Y. However, extensive spectral characterization of this material has revealed that the trimer, "ruthenium red", has been formed on the zeolite support: $[(NH_3)_5Ru^{III}-O-Ru^{IV}(NH_3)_4-O-Ru^{III}(NH_3)_5]^{6+}$–Y. Heat treatment of the $[Ru(NH_3)_5N_2]^{2+}$–Y species under vacuum produced a highly reactive ruthenium species, designated Ru^{ac}–Y, which chemically reacted with CO, NH_3, and NO. The reaction with NH_3 indicated that a Brønsted acid site interaction in the zeolite was involved. The reaction with CO could be interpreted as interaction with metal ion sites in the zeolite supercages. The absence of a CO–cation specific infrared band indicated that the oxidation state of the ruthenium in Ru^{ac}–Y is probably less than 2, i.e., small clusters such as Ru_n^0 or Ru_n^+. The reaction of the active species and NO produced a material containing coordinated nitrosyl. No reaction could be observed for molecular nitrogen, H_2S, or SO_2.

Introduction

Noble metals and their complexes supported on a variety of "inert" materials have been used as heterogeneous catalysts in a variety of reactions.[1,2] Ruthenium-containing catalysts have been found to be very versatile, their properties ranging from a pronounced selectivity for the reduction of nitrogen oxides to molecular nitrogen[3–8] to a high specific activity for the carbon monoxide–hydrogen methanation reaction.[9–12] Ruthenium complexes have also been used as homogeneous catalysts in the water gas shift reaction to produce hydrogen.[13] Thus the practical potential of ruthenium catalysts range from the control of nitrogen oxide emissions to the gasification of coal. At the present time, the mechanisms for the ruthenium catalysts are only partially understood, and detailed characterization data for the catalyst materials are still quite limited. The chemistry of ruthenium is unique among the platinum metals in that it exhibits a range of stable oxidation states (from 0 to +8), it forms an almost unlimited number of complex molecules, and it has a pronounced tendency to form multinuclear complexes where ruthenium atoms are bridged by a variety of atomic and molecular ligands. This versatility of chemical reactivity is both an advantage, in terms of the variety of chemical reactions which are possible, and a problem, in that most ruthenium reaction systems are complex, and the maintenance of a particular species or oxidation state can be quite difficult. An example of this behavior as applied to ruthenium catalysts is exhibited in the so-called "dual state" behavior where the catalytic activity of dispersed ruthenium metal is enhanced by exposure to oxygen.[14] The potential utility of supported, heterogeneous ruthenium catalysts and the rich ruthenium chemistry associated with such materials provides a challenge to the experimental chemist to specifically characterize the catalytic materials and

*To whom correspondence should be addressed at Division of Engineering Research, Louisiana State University, Baton Rouge, LA 70803.

to relate the catalytic activity to the physical and chemical properties of the metal and its supports. This paper presents the continuation of our studies on the physical properties and chemical reactivity of complex ruthenium cations supported on Y-type zeolites.

Previous studies[15] have indicated that the $[Ru(NH_3)_5N_2]^{2+}$ ion can be incorporated into a Y-type zeolite by simple cation exchange. The reactivity of the ion supported on the zeolite was found to be significantly different from that observed for the ion in aqueous solution. Initial conclusions derived from ^{99}Ru Mössbauer data were that the ion was readily oxidized by atmospheric oxygen, higher oxidation-state species could be obtained by heating the supported material under vacuum, and the reduced metallic state readily reacted with small molecular species such as NH_3 and NO. An analysis of the quadrupole splitting parameter for the exchanged $[Ru(NH_3)_5N_2]^{2+}$ after evacuation indicated a change in structure of the ion upon incorporation into the zeolite. The increased ΔE_Q could be rationalized by either assuming that molecular nitrogen was lost on evacuation or assuming that the ion was distorted from its near O_h symmetry by the effective oxide sites within the zeolite cavity. The wine red oxidation product was thought to be $[Ru(NH_3)_5OH]^{2+}$.[15-17] Reduction of the complex ion by H_2 at 400 °C produced finely divided ruthenium metal which was readily oxidized and which did not exhibit ruthenium lines in the X-ray diffraction pattern, indicating that the particles were less than 80 Å in diameter.[15] However, no detailed analysis of the specific chemical reactions involved has been carried out. This report presents UV–visible and infrared spectral data for the reactants and products of the various reactions exhibited by the zeolite-supported ruthenium complex. These results provide the information required to identify the wine red air-oxidation product and to deduce the chemical identity of the reaction products of the reactive ruthenium species (produced by heating the exchanged complex–zeolite under vacuum) with CO, NH_3, NO, N_2, H_2S, and SO_2. The CO interactions are particularly important since the adsorptivity of CO has been used as a surface probe in the study of zeolite surfaces.[18,19] The reactions with ammonia are also significant in that they may provide information on the surface acidity of the zeolite by determining whether the NH_3 molecule occupies a Brønsted acid, a Lewis acid, or a cation site.[18]

Experimental Methods

Materials. Na–Y zeolite (SK-40 Lot No. 3606-385) was obtained from the Linde Co. Ruthenium trichloride trihydrate was purchased from Engelhard Industries. Matheson NO was purified by repeated distillation at the melting point of acetone (−95 °C) to remove N_2O and NO_2. Dissolved N_2 was eliminated by freezing the NO at liquid nitrogen temperature (−196 °C), evacuating for 5 min, and removing the liquid N_2. The first portion of NO was pumped off and the remainder stored in a 500-mL flask for use. Matheson CO (99.5%), anhydrous NH_3, and N_2 were purified by being passed through a trap at −196 °C before use. Matheson SO_2 and H_2S (CP grade) were used as received. All other chemicals used were reagent grade.

Preparation of $[Ru(NH_3)_5N_2]I_2$. Attempts to prepare $[Ru(NH_3)_5N_2]Cl_2$ by the method of Lin and Schreiner[20] produced products containing a nitrosyl impurity (IR band at 1892 cm^{-1}). Allen's method,[21] which involved treating ruthenium trichloride (1 g) dissolved in water (12 mL) with hydrazine hydrate (10 mL), gave a product contaminated with hydrazine (IR bands at 945 and 1145 cm^{-1}).[22] Attempts were made to remove the hydrazine impurity in the dinitrogen complex by reducing the amount of hydrazine hydrate in the preparation step. By trial and error it was found that the following experimental conditions gave pure $[Ru(NH_3)_5N_2]I_2$. Ruthenium trichloride (1 g) was dissolved in water (10 mL), and hydrazine hydrate (1 mL) was added dropwise. The reaction mixture was stirred overnight, followed by the addition of H_2O (5 mL) and hydrazine hydrate (4 mL). The mixture was stirred for 2 h and filtered. A saturated aqueous solution of NH_4I was added dropwise to the filtrate to precipitate the iodide salt. The reaction flask was kept in the

refrigerator for 2 h before filtering. The $[Ru(NH_3)_5N_2]I_2$ precipitate was washed with H_2O, absolute ethyl alcohol, and ether and dried under vacuum; yield, 0.7 g (39% based on ruthenium). Anal. Calcd for $RuN_7H_{15}I_2$: Ru, 21.58; NH_3, 18.16. Found: Ru, 21.63; NH_3, 17.82.

The precipitation of the $[Ru(NH_3)_5N_2]^{2+}$ ion as the iodide salt is advantageous because of its insolubility. The more soluble chloride salt is much more difficult to prepare without the inclusion of solution impurities or the chance of ligand exchange. The variation in the amount of hydrazine needed to reduce the aqueous ruthenium trichloride is probably a function of the particular sample. It has long been known that commercial $RuCl_3 \cdot xH_2O$ in aqueous solution contains a mixture of polynuclear aquochloro complexes of Ru(III) and Ru(IV), with earlier materials being primarily Ru(IV).[23,24] Thus, the appropriate ruthenium trichloride–hydrazine ratio needed to prepare hydrazine-free complexes may need to be assessed for each batch of ruthenium trichloride.

Preparation of Ruthenium Red. The trimer ruthenium red, $[(NH_3)_5Ru^{III}-O-Ru^{IV}(NH_3)_4-O-Ru^{III}(NH_3)_5]^{6+}$, was prepared by the method described by Fletcher and co-workers.[23] Purity and absence of oxidation were ascertained by UV–visible spectral characterization of the material in the solid and in aqueous solution.

Exchange Procedure. Cation exchange of the dinitrogen and ruthenium red complexes into the Na–Y zeolite was performed as earlier described by Clausen and Good.[15] The ruthenium complexes (approximately 0.5 g) in deoxygenated H_2O (100 mL) were treated with Na–Y zeolite (1 g), and the reaction mixture was stirred for 16 h under argon atmosphere. The zeolite in each case was filtered, washed with distilled H_2O, and dried over P_2O_5 under vacuum in a desiccator. The filtrate was analyzed for remaining ruthenium and for the exchanged sodium ion. Total ruthenium remaining in the filtrate was determined gravimetrically by oxidation to RuO_2. Total exchanged sodium was determined by the classical uranyl acetate method. Typical results were

$[Ru(NH_3)_5N_2]I_2$ exchange

by Na analysis 60 ± 1% } 0.098 g of Ru/g of Y zeolite
by Ru residue 59 ± 1.5%

Ru-red exchange

by Na analysis 40 ± 1% } 0.066 g of Ru/g of Y zeolite
by Ru residue 39 ± 1.5%

X-ray diffraction patterns of the exchanged samples indicated that there was no observable loss of zeolite crystallinity.

Gas Reactions. In one set of experiments, the exchanged complex, $[Ru(NH_3)_5N_2]^{2+}$–Y, was heated to 400 °C at 10^{-5} torr for 30 min and cooled to 25 °C under vacuum to give a highly reactive, black, powdered species which is designated as Ru^{ac}–Y. The Ru^{ac}–Y sample was treated separately with air and a variety of gases such as NH_3, CO, N_2, H_2S, and SO_2 (flow systems; flow rates of 40 mL/min) and NO (static system; 35 torr) at 25 °C for 30 min. Samples prepared external to the infrared cell were handled in an inert atmosphere. Infrared spectra were obtained on these treated samples in KBr disks. In a second set of experiments, the above procedures were repeated with a $[Ru(NH_3)_5N_2]^{2+}$–Y wafer in the IR cell. The construction of the IR cell was similar to that of the one described by Brown et al.[25] The cell was made of Pyrex glass with NaCl windows fixed by Glyptal (1201 red enamel insulating paint, General Electric Co., Schenectady, NY). The furnace section of the cell consisted of a heating tape wound around the cell and covered with asbestos. The temperature was measured by a thermocouple. The zeolite wafer containing the exchanged ruthenium complex was prepared by spreading the zeolite powder (20–30 mg) between stainless steel plates and then compressing it at 15 000 lbs/in.[2]. The wafer was inserted into an aluminum pellet holder which was suspended in the IR cell by a gold wire. By rotation of the crank at the top of the cell, the wafer could be positioned in the upper furnace section to record the IR spectrum on a Perkin-Elmer 283 spectrophotometer. The cell was connected to a conventional Pyrex glass vacuum system. Identical results were obtained for the KBr-disk samples and the zeolite wafers. Infrared spectra were obtained on blank samples containing Na–Y zeolite (pretreatment: 400 °C at 10^{-5} torr for 30 min and then cooled to 25 °C) that were treated with CO, NO, and NH_3 exactly in the same manner as described above.

UV–Visible Spectra. All reported spectra were taken on a Cary Model 17 spectrophotometer. Spectra of solids were obtained by

Table I. Infrared Spectral Data for Ruthenium-Exchanged Zeolites

sample no.	treatment	band position, cm^{-1}	assignment
1A (Na-Y)	nil	1635	$\delta(H_2O)$
1B	1A heated to 400 °C at 10^{-5} torr for 30 min	1635	$\delta(H_2O)$
1C	1B exposed to NH$_3$ at 25 °C for 30 min	1635	$\delta(H_2O)$
1D	1B exposed to NO at 25 °C for 30 min	1635	$\delta(H_2O)$
1E	1B exposed to CO at 25 °C for 30 min	1635	$\delta(H_2O)$
2A [Ru(NH$_3$)$_5$N$_2$]$^{2+}$–Y	nil	2104	$\gamma(NN)$
		1630	$\delta(NH_3, deg) + \delta(H_2O)$
		1318	$\delta(NH_3, sym)$
2B	sample 2A exposed to air at 25 °C for 20 min (one scan)	2103	$\gamma(NN)$
		1863	$\gamma(NO)$
		1635	$\delta(NH_3, deg) + \delta(H_2O)$
		1449	$\delta(NH_4{}^+)$
		1323	$\delta(NH_3, sym)$
2C	sample 2B exposed to air at 25 °C for 9 days	2103 (decreasing)	$\gamma(NN)$
		1863 (increasing)	$\gamma(NO)$
		1635	$\delta(NH_3, deg) + \delta(H_2O)$
		1449	$\delta(NH_4{}^+)$
		1323	$\delta(NH_3, sym)$
2D	sample 2C reduced in H$_2$ at 150 °C for 5 h	1635	$\delta(H_2O)$
		1449	$\delta(NH_4{}^+)$
2E	sample 2A heated to 100 °C at 10^{-5} torr for 3 h	1635	$\delta(H_2O)$
		1400	$\delta(NH_4{}^+)$
2F	sample 2A heated to 400 °C at 10^{-5} torr for 30 min	1630	$\delta(H_2O)$
2G	sample 2F exposed to NH$_3$ at 25 °C for 30 min	3450, 3180	$\gamma(NH_4{}^+)$
		1630	$\delta(H_2O)$
		1400	$\delta(NH_4{}^+)$
2H	sample 2F exposed to NO at 25 °C for 30 min	1862	$\gamma(NO)$
		1628	$\delta(H_2O)$
2I	sample 2F exposed to CO at 25 °C for 30 min	2132, 2054	$\gamma(CO)$
		1635	$\delta(H_2O)$

preparing Nujol mulls on filter paper.

Results and Discussion

Reaction of [Ru(NH$_3$)$_5$N$_2$]$^{2+}$–Y with Air. A neat wafer of the pale yellow [Ru(NH$_3$)$_5$N$_2$]$^{2+}$–Y was exposed to air for 9 days and its IR spectra monitored at different intervals of time. The results as indicated by the major infrared bands are shown in Table I. After one scan (a period of a few minutes), the color of the wafer started changing to wine red; the intensity increased with time. The intensity of the ν(NN) band in the infrared region decreased with time while new bands appeared at 1863 cm^{-1} [ν(NO); intensity increased with time] and at 1449 cm^{-1} due to δ(NH$_4{}^+$). However, all of the coordinated N$_2$ was not completely removed even after the full 9 days' exposure to air.

The appearance of the band at 1449 cm^{-1} can best be rationalized in terms of an NH$_3$ molecule from the metal complex interacting with a Brønsted acid site on the zeolite to produce NH$_4{}^+$. Ammonia interactions with Brønsted acid, Lewis acid, and cation sites in zeolites have been previously characterized by infrared spectroscopy.[18] Generally, ammonia adsorbed on zeolite gives rise to two separate infrared bands, one at 1475 cm^{-1} attributable to δ(NH$_4{}^+$) (the Brønsted site interaction) and another at 1630 cm^{-1} which results from the Lewis acid site interactions (N–Al) and the cation center interaction. The band at 1635 cm^{-1} (Table I) coincides with the bending vibration of H$_2$O so that no conclusions can be drawn about the ammonia interactions at the Lewis acid or cation sites.

Clausen and Good[15] and Laing et al.[16] suggested that the exchanged dinitrogen complex decomposed in air to form [Ru^{III}(NH$_3$)$_5$OH]$^{2+}$–Y. These workers based their conclusions on the work of Sigwart and Spence,[17] who produced the red [Ru^{III}(NH$_3$)$_5$OH]$^{2+}$ ion (UV band at 290 nm) by the photochemical oxidation of [Ru(NH$_3$)$_5$N$_2$]$^{2+}$ in neutral solution. We have now repeated the photochemical oxidation of the dinitrogen complex in our laboratory by exposing a sample of [Ru(NH$_3$)$_5$N$_2$]$^{2+}$ in neutral solution to a 300-nm mercury lamp for 45 min. Indeed, the [Ru^{III}(NH$_3$)$_5$OH]$^{2+}$ species with
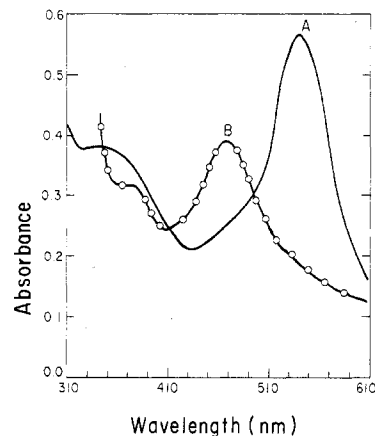

Figure 1. Visible spectra: A, wine red complex in 1 N NaCl; B, oxidized brown complex in 0.1 N HNO$_3$.

a UV band at 292 nm was formed. However, this UV band at about 290 nm was not observed in the spectrum of the wine red oxidation species produced from the air exposure of [Ru(NH$_3$)$_5$N$_2$]$^{2+}$–Y. Nujol mulls of the solid material and the wine red solution eluted from the Sephadex column (see details outlined below) both exhibited a broad band in the visible region of the spectrum. This band and the general shape of the UV–visible spectrum for the wine red species are very similar to the spectral characteristics reported for "ruthenium red",[23] [(NH$_3$)$_5$Ru^{III}–O–Ru^{IV}(NH$_3$)$_4$–O–Ru^{III}-(NH$_3$)$_5$]$^{6+}$.

To verify the designation of the wine red oxidation product as "ruthenium red", we undertook further characterization of the species in solution as described by Fletcher et al.[23] in their original definition of the red ruthenium trimer. The wine red solution was made acidic with 0.1 N HNO$_3$ solution, and the color changed to brown. The resulting spectrum is shown as curve B in Figure 1. This brown solution (λ_{max} at 468 nm) compares with the brown complex (λ_{max} at 460 nm) referred to by Fletcher and co-workers as "ruthenium brown",

$[(NH_3)_5Ru^{IV}-O-Ru^{III}(NH_3)_4-O-Ru^{IV}(NH_3)_5]^{7+}$, the one-electron oxidation product of ruthenium red. The brown solution could be converted back to the wine red solution by making the solution alkaline with 0.1 N NaOH. The Mössbauer parameters reported previously for this species are not inconsistent with this conclusion.[15] The spectrum for the $[Ru(NH_3)_5N_2]^{2+}$-Y after exposure to air for 2 days exhibited a broad, poorly resolved band with a line width of 0.79 mm/s and an isomer shift of -0.37 mm/s. The Mössbauer spectrum of a pure, solid sample of ruthenium red exhibits a broad absorption which can be computer resolved into two sets of doublets.[26] However, the maximum absorption occurs at approximately -0.37 mm/s, and the appropriate line width of the absorption envelope is 0.72 mm/s. Further verification of the $[Ru(NH_3)_5N_2]^{2+}$ oxidation product was undertaken by carrying out a series of exchange reactions as outlined below.

A sample (0.2 g) of $[Ru(NH_3)_5N_2]^{2+}$-Y was exposed to air at 25 °C for 2 days. The resulting wine red sample was treated with 15 mL of 1 N NaCl solution and stirred for 15 min. The solution containing the wine red cation was filtered. The visible spectrum (curve A) of the filtrate is shown in Figure 1 (λ_{max} at 542 nm). The UV spectrum (not shown) did not exhibit the 290-nm absorption band characteristic of the $[Ru^{III}(NH_3)_5OH]^{2+}$ species.[17]

Three infrared spectra of neat wafers of $[Ru(NH_3)_5N_2]^{2+}$-Y were taken successively at 30-min intervals under atmospheric conditions. At the end of the first scan, the pale yellow color of the exchanged complex showed a pink tinge, and at the end of the third scan, the wafer had turned completely wine red. This wafer was treated with 15 mL of 1 N NaCl solution, and the mixture was stirred for 15 min and filtered. The wine red filtrate was placed on a Sephadex C-50 cation exchanger (particle size 40–120 μm; Pharmacia Fine Chemicals Inc., NJ) column (13-cm length, 2.3-cm diameter) and eluted with 1 N NaCl solution. The first, pale yellow, band that came off the column with 15 mL of NaCl was identified as unreacted $[Ru(NH_3)_5N_2]^{2+}$ as shown by its UV absorption band at 221 nm. The second, pink (or wine red), band was eluted with 40 mL of 2 N NaCl and exhibited a visible spectrum whose features (λ_{max} at 542 nm) were identical with those of the spectrum shown in Figure 1. The UV spectrum again did not show the 290-nm band characteristic of $[Ru^{III}(NH_3)_5OH]^{2+}$. The third, brownish red, band at the top of the column could not be eluted with 100 mL of 2 N NaCl. Although the identity of this species has not been conclusively determined, the experimental results given below indicate that this material is probably ruthenium brown. The Nujol mull, solid-state visible spectrum of the initial wine red zeolite wafer exhibited a spectrum of the same general shape as that given above for the wine red solution. However, the prominent visible peak was shifted to a λ_{max} of 558 nm. As indicated below for a verified ruthenium red sample, this shift is apparently a consequence of the media change. Again, no UV band in the vicinity of 290 nm was observed.

The conversion of the monmeric $[Ru(NH_3)_5N_2]^{2+}$ species to the ruthenium red trimer is somewhat surprising in view of the pore sizes of the zeolite. To further investigate this phenomenon, some exchange experiments were performed by using pure, freshly prepared ruthenium red. As indicated in the Experimental Section, a 40% exchange of cation sites was achieved. Figure 2 indicates the results of these experiments. Curve E is the aqueous solution spectrum of the pure Ru-red starting material and indicates the characteristic λ_{max} at 540 nm. Curve B is the Nujol solid-state spectrum of a freshly prepared Ru-red-Y sample with a λ_{max} at 555 nm, corresponding to the solid-state visible spectrum of the $[Ru(NH_3)_5N_2]^{2+}$ oxidation product shown in curve A. The reality of this media shift of λ_{max} for Ru-red is further supported by
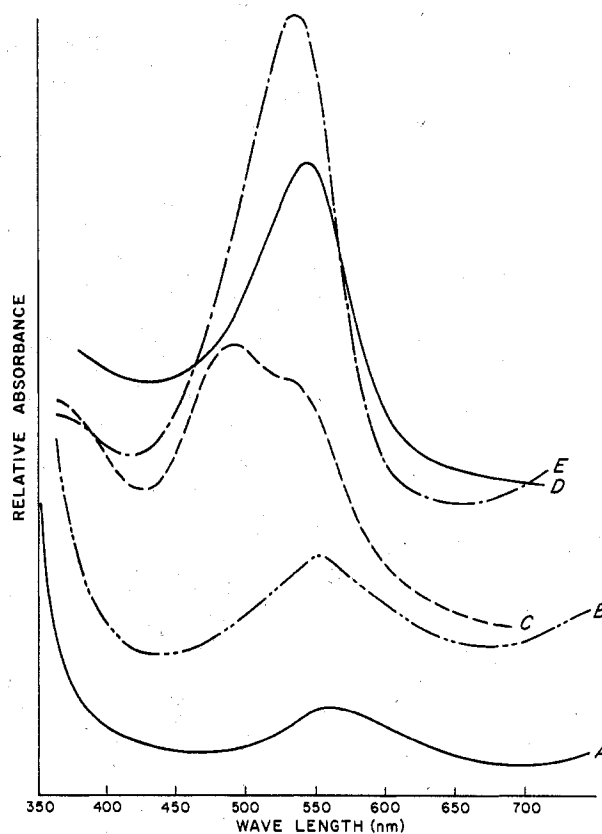

Figure 2. Visible spectra of ruthenium species: A, $[Ru(NH_3)_5N_2]^{2+}$-Y exposed to air and light for 48 h; B, Ru-red-Y freshly prepared; C, Ru-red-Y exposed to air and light for 48 h; D, Ru-red in aqueous solution reextracted from Ru-red-Y by 2 N NaCl; E, aqueous solution spectrum of pure Ru-red starting material.

the fact that the spectrum of a pure, solid sample of the Ru-red in Nujol exhibited a λ_{max} at 553 nm. Curve C is the spectrum of a sample of Ru-red-Y which had been exposed to air and light. Note the appearance of the new peak at 490 nm which can be assigned to the oxidation product Ru-brown. Curve D is the spectrum of the filtrate from a 2 N NaCl extraction of the Ru-red-Y. The λ_{max} is at 540 nm, the characteristic absorption maximum for Ru-red in aqueous solution.

In summary, the $[Ru(NH_3)_5N_2]^{2+}$-Y species reacts with air to form a mixture of products. Some coordinated N_2 is lost from the complex, and some coordinated NH_3 is released into the zeolite framework where it forms NH_4^+ at a Brønsted acid site. The resulting complex fragments interact with atmospheric oxygen to form the oxygen-bridged ruthenium trimer, ruthenium red, where the formal oxidation state of the ruthenium has been increased from Ru(II) to a mixture of Ru(III) and Ru(IV).[15,23] The ready formation of this trimer indicates either that several $[Ru(NH_3)_5N_2]^{2+}$ ions are exchanged into the large cavities of the zeolite in close proximity to one another or that there is significant mobility of the exchanged complex ion within the zeolite structure. The studies of Lunsford and co-workers[12] on the particle sizes of the ruthenium clusters resulting from the reduction of $[Ru(NH_3)_6]^{3+}$ exchanged into a Y-type zeolite and a similar study by Coughlan et al.[27] for exchanged $[Ru(H_2O)_6]^{3+}$ argue strongly for the idea that the complexes are exchanged into (and remain during reaction) the large cavities of the zeolite. In any case, the zeolite acts as a catalyst in the oxidation reaction since $[Ru^{II}(NH_3)_5N_2]^{2+}$ is stable to atmospheric oxygen both in aqueous solution and in the bulk solid state.

The ready exchange of the Ru-red trimer into the zeolite at a 40% cation site exchange level needs further investigation. Since only about 10% of the exchange sites are on the external

surface of the zeolite,[18] these sites cannot accommodate all of the exchanged trimer. The backbone structure of Ru-red, Ru–O–Ru–O–Ru, is linear;[26] thus the molecule may penetrate the large cavities. However, the determination of precise physical accommodation of this large cation in the zeolite framework will have to await a single-crystal X-ray analysis.

In addition to the major oxidation product described above, the air oxidation of $[Ru(NH_3)_5N_2]^{2+}$–Y produces a small amount of a nitrosyl complex, most probably $[Ru^{II}-(NH_3)_5NO]^{3+}$–Y, which was exchanged off the zeolite support by 1 N NaCl but could not be subsequently eluted from a Sephadex column by 2 N NaCl.

After treatment with H_2 gas at 150 °C for 5 h, infrared analysis indicates that all of the coordinated N_2, NH_3, and NO^+ have been removed from the oxidation product mixture (see Table I). The liberated NH_3 is trapped on the Brønsted acid sites in the zeolite as indicated by the appearance of the strong infrared band at 1449 cm^{-1}. Our previous Mössbauer data[15] would indicate that the ruthenium species have been reduced to metallic ruthenium although the precise reduction conditions used here are different. Further Mössbauer data on several of these systems are now being collected and will be published in a subsequent paper.

Decomposition of $[Ru(NH_3)_5N_2]^{2+}$–Y by Heat and Vacuum and the Formation of Ru^{ac}–Y. In our initial Mössbauer studies,[15] we observed that the quadrupole splitting of the $[Ru(NH_3)_5N_2]^{2+}$ ion was increased from 0.22 mm/s in the bulk $[Ru(NH_3)_5N_2]Cl_2$ to 0.56 mm/s in the exchanged zeolite although the isomer shift remained essentially constant. Since the spectrum was taken on an exchanged sample which had been dried and evacuated to 10^{-5} torr at 25 °C, it was suggested that the increase in quadrupole splitting could be due either to the loss of coordinated N_2 to form an asymmetric, five-coordinated species as suggested by Laing et al.[16] or to the distortion of the complex by virtue of its exchange site in the rigid aluminosilicate structure of the zeolite. To decide between these two possibilities, we investigated the infrared spectra of the evacuated sample. After evacuation at 10^{-5} torr for 2 days, the intense ν(NN) band remained, indicating that the molecular N_2 was not removed. Thus it appears that the metal complex ion is distorted by its attachment to the zeolite structure. Other authors have indicated that cations exchanged into a zeolite can occupy several different sites within the zeolite framework.[28–30] Each site could be expected to impose its own characteristic structural and electronic requirements on the cation. A recent study of Ag$^+$-exchanged zeolite A[31] has shown that $[Ag_2(N_3H_5)_3]^{2+}$ and $[Ag(N_3H_3)]^+$ are stabilized by extensive hydrogen bonding of the nitrogen hydrides to the zeolite framework. Similar hydrogen bonding of some or all of the ammonia hydrogen atoms to oxygen sites in $[Ru(NH_3)_5N_2]^{2+}$–Y would account for the increased quadrupole splitting.

The removal of coordinated N_2 from the exchanged ruthenium complex could be accomplished [as monitored by the disappearance of the 2104-cm^{-1} ν(NN) band in the infrared] by heating the sample at 100 °C at 10^{-5} torr for 3 h. In addition, a new band at 1400 cm^{-1} (δ(NH$_4^+$)) appeared, indicating some loss of coordinated NH_3. As observed in our earlier study,[15] if the sample was heated at 400 °C at 10^{-5} torr for 4 h, both the coordinated N_2 and NH_3 were removed (see Table I) and a highly reactive ruthenium species was formed in the zeolite. This reactive species, designated Ru^{ac}–Y, exhibited Mössbauer parameters of 0.06 mm/s for the isomer shift and 0.43 mm/s for the quadrupole splitting. The isomer shift is indicative of ruthenium metal or ruthenium in the IV or V oxidation state, although bulk ruthenium metal does not exhibit quadrupole splitting.[32] The formation of the oxidized ruthenium trimer discussed earlier, the observation by Seff
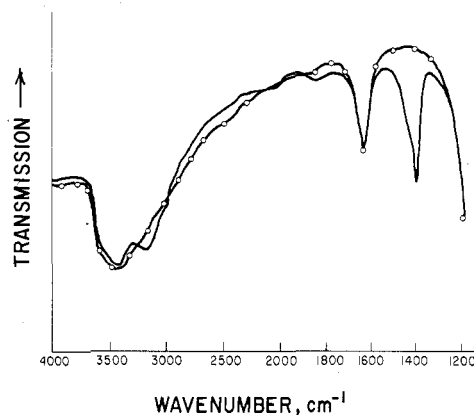

Figure 3. Infrared spectra: Ru^{ac}–Y (–O–) and Ru^{ac}–Y exposed to NH$_3$ (—).

and co-workers[33] that Ag$^+$ is reduced by oxide ions of the zeolite framework to form small (Ag$_6$) metal clusters, and the work of Lunsford et al.[12] argue strongly for the formation of small ruthenium metal clusters or stabilized metal clusters coordinated to metallic ions. The Mössbauer spectrum is consistent with either a small metal cluster of low symmetry (as compared to bulk ruthenium metal) or a small metal cluster coordinated to Ru(IV) sites in the zeolite. Further work will be required to decide between these two possibilities. Comparative magnetic measurements and crystallographic studies are being developed in our laboratory for the further characterization of these Ru^{ac}–Y species.

Reaction of Ru^{ac}–Y with Small Molecular Gases. The reactions of Ru^{ac}–Y with NH_3, CO, NO, N_2, H_2S, and SO_2 were monitored by infrared analysis. The results are shown in Table I. Although the first three gases strongly interacted with the supported ruthenium species, no interactions of N_2, H_2S, or SO were observed.

The interaction of NH_3 with Ru^{ac}–Y produced the infrared spectrum shown in Figure 3. The band assignments are 3450 and 3180 cm^{-1} to NH$_4^+$ stretching vibrations and 1400 cm^{-1} to the NH$_4^+$ bending vibration. As indicated earlier, the only NH$_4^+$ vibrational mode discernible in the spectrum of oxidized $[Ru(NH_3)_5N_2]^{2+}$ was the bending mode at 1449 cm^{-1}. No bands attributable to NH$_4^+$ were observed in the spectrum of the sodium Y zeolite blank treated with gaseous ammonia.

The NH$_4^+$ bands persisted in the spectrum of the NH_3 treated Ru^{ac}–Y when the sample was evacuated at 10^{-5} torr at ambient temperature for 2 h. To completely remove the adsorbed NH_3, it was necessary to heat the sample to 400 °C under vacuum for 30 min. These results indicate that the NH_3 molecule reacts with the Ru^{ac}–Y at a Brønsted acid site in the zeolite (the origin of the strong ir band at 1440 cm^{-1}) probably through chemisorption on the active ruthenium. The presence of the H_2O band at 1630 cm^{-1} again precludes the possibility of monitoring interactions at Lewis acid and cation sites. These results are consistent with the Mössbauer parameters observed earlier for the Ru^{ac}–Y species after reaction with NH_3.[15] The isomer shift of the ruthenium changed from –0.06 mm/s for Ru^{ac}–Y to –0.25 mm/s for the NH$_3$-treated material. These results indicate chemisorption of the NH_3 on the ruthenium to form a new complex species.

Nitric oxide reacted with Ru^{ac}–Y to produce a species exhibiting an infrared band at 1862 cm^{-1}. This band is assignable to the stretching frequency of coordinated NO$^+$ in the normal linear Ru^{II}–NO moiety.[18,34–36] No reaction was observed between NO and the Na–Y blank. No disproportionation products such as N_2O, N_2O_3, or NO_2 were observed as reported by Chao and Lunsford.[37] The formation of a Ru–NO entity in the Ru^{ac}–Y sample is again consistent with the Mössbauer results for other ruthenium–nitrosyl moie-

ties.[15,32,36] Again it was necessary to heat the sample to 400 °C under vacuum to expel the NO.

The interaction of CO with Ru^{ac}–Y produced a species which exhibited CO infrared bands at 2132 and 2054 cm^{-1} as shown in Table I. To assess the molecular (or molecular fragments) structure(s) of the metal–carbonyl species it is necessary to briefly review some of the structural parameters of the Y-type zeolites. Although the Faujasite Y-type zeolites have three types of exchangable cation sites or cages, only the supercage is large enough (diameter of 13 Å with a channel opening of 8–9 Å) to accommodate large complex cations such as the [Ru(NH$_3$)$_5$N$_2$]$^{2+}$ species.[18,19,38,39] The diameter of a rotating CO molecule has been estimated to be 4.5 Å.[40,41] Thus one would expect CO to interact with sites in the supercages, and CO can be used to probe the cationic or metallic sites in the zeolite.[18] Another diagnostic property of the CO is that the molecule reacts with multivalent cations, but not monovalent ones, to form a species which exhibits a cation-specific band around 2200 cm^{-1}.[19] This last test was used to show that the Ca^{2+} ions in 35% exchanged CaX zeolite were in the small volume, "hidden", hexagonal prism sites (site I).[19] In the present case about 60% of the cation sites were exchanged with [Ru(NH$_3$)$_5$N$_2$]$^{2+}$ providing about 17 ruthenium atoms per unit cell. The Ru^{ac}–Y formed from the [Ru(NH$_3$)$_5$N$_2$]$^{2+}$–Y reacted with CO as indicated above, but the infrared spectrum of the product did not contain the cation-specific band around 2200 cm^{-1}. This result, coupled with the appearance of the 2132 and 2054 cm^{-1} bands, indicates that the ruthenium species occupy the supercages in the zeolite and have cationic charges of less than two. These results are consistent with the conclusion drawn earlier that the ruthenium species in Ru^{ac}–Y are probably small clusters such as Ru$_n^0$ or Ru$_n^+$.

The infrared bands at 2132 and 2054 cm^{-1} can best be assigned to the symmetric and antisymmetric stretching frequencies of two CO molecules bonded to a single ruthenium site as indicated by Davydov et al.[35,42] These workers proposed the structure
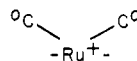
for the species formed by the interaction of CO on an oxidized ruthenium surface supported on silica. The spectrum of their CO–Ru product was very similar to that observed here for the reaction product of Ru^{ac}–Y and CO, lending some support to an assignment of Ru$_n^+$ for Ru^{ac}. Again the CO could be removed only after heating the sample at 400 °C at 10^{-5} torr.

Conclusions

The [Ru(NH$_3$)$_5$N$_2$]$^{2+}$ ion is exchanged intact into the supercages of a Y-type zeolite where it is probably hydrogen bonded through the hydrogens on NH$_3$ to oxide sites in the cage. The resulting [Ru(NH$_3$)$_5$N$_2$]$^{2+}$–Y is easily oxidized to the Ru^{III}–Ru^{IV} trimer, ruthenium red, by ambient atmospheric oxygen. The [Ru(NH$_3$)$_5$N$_2$]$^{2+}$–Y species can be converted to an active, supported ruthenium species by evacuating the sample at 10^{-5} torr at 400 °C. The characterization of the resulting Ru^{ac}–Y indicates that ruthenium probably exists as small ruthenium clusters of zero or low positive charge. The interaction of NH$_3$, NO, and CO with this material produces identifiable M–X species which decompose only at fairly high

temperatures. The UV–visible and infrared spectral results reported in this paper complement the Mössbauer parameters obtained previously for these materials, and the combination of the data provides fairly detailed insight into their chemical nature. The precise structures of the ruthenium clusters and the Ru–X addition compounds are still unknown, and additional magnetic, crystallographic and Mössbauer studies are underway in our laboratory to more clearly define the chemical and structural details of these materials.

References and Notes

(1) Peterson, R. J. "Hydrogenation Catalysts" (Chemical Technology Review No. 94); Noyes Data Corp.: Park Ridge, NJ, 1974.
(2) Hartley, F. R.; Venzey, P. N. *Adv. Organomet. Chem.* **1977**, *15*, 189.
(3) Shelef, M.; Gandhi, H. S. *Ind. Eng. Chem., Prod. Res. Develop.* **1972**, *11*, 393.
(4) Klimisch, R. L.; Taylor, K. C. *Environ. Sci. Technol.* **1973**, *7*, 127.
(5) Otto, K.; Shelef, M. *Z. Phys. Chem. (Frankfurt am Main)* **1973**, *85*, 308.
(6) Shelef, M.; Gandhi, H. S. *Platinum Met. Rev.* **1974**, *18*, 2.
(7) Kuo, J. C. W.; Morgan, C. R.; Lassen, H. G. *SAE [Tech. Pap.]* **1971**, No. 710289.
(8) Clausen, C. A., III; Good, M. L. *J. Catal.* **1977**, *46*, 58.
(9) Vannice, M. A. *J. Catal.* **1975**, *37*, 449.
(10) Vannice, M. A. *J. Catal.* **1975**, *37*, 462.
(11) Vannice, M. A. *J. Catal.* **1975**, *40*, 129.
(12) Elliott, D. J.; Lunsford, J. H. *J. Catal.* **1979**, *57*, 11.
(13) Laine, R. M.; Rinker, R. G.; Ford, P. C. *J. Am. Chem. Soc.* **1977**, *99*, 252.
(14) Taylor, K. C.; Sinkevitch, R. M.; Klimisch, R. L. *J. Catal.* **1974**, *35*, 34.
(15) Clausen, C. A., III; Good, M. L. *Inorg. Chem.* **1977**, *16*, 816.
(16) Laing, K. R.; Leubner, R. L.; Lunsford, J. H. *Inorg. Chem.* **1975**, *14*, 1400.
(17) Sigwart, C.; Spence, J. T. *J. Am. Chem. Soc.* **1969**, *91*, 3991.
(18) Ward, J. W. *ACS Monogr.* **1976**, No. 171.
(19) Angell, C. L.; Schaffer, P. C. *J. Phys. Chem.* **1966**, *70*, 1413.
(20) Lin, S. W.; Schreiner, A. F. *Inorg. Nucl. Chem. Lett.* **1970**, *6*, 561.
(21) Allen, A. D.; Bottomley, F.; Harris, R. O.; Reinsalu, V. P.; Sennoff, C. V. *J. Am. Chem. Soc.* **1967**, *89*, 5595.
(22) Chatt, J.; Richards, R. L.; Fergusson, J. E.; Love, J. L. *Chem. Commun.* **1968**, 1522.
(23) Fletcher, J. M.; Greenfield, B. F.; Hardy, C. J.; Scargill, D.; Woodhead, J. L. *J. Chem. Soc.* **1961**, 2000.
(24) Fletcher, J. M. *J. Inorg. Nucl. Chem.* **1958**, *8*, 277.
(25) Brown, M. F.; Gonzalez, R. D. *J. Phys. Chem.* **1976**, *80*, 1731.
(26) Clausen, C. A., III; Prados, R. A.; Good, M. L. *Inorg. Nucl. Chem. Lett.* **1971**, *7*, 485.
(27) Coughlan, B.; Narayanan, S.; McCann, W. A.; Carrol, W. M. *J. Catal.* **1977**, *49*, 97.
(28) Smith, J. V. *Adv. Chem. Ser.* **1971**, No. *101*, 171.
(29) Olson, D. H. *J. Phys. Chem.* **1970**, *74*, 2758.
(30) Vansant, E. F.; Lunsford, J. H. *J. Phys. Chem.* **1972**, *76*, 2860.
(31) Kim, Yang; Gilje, J. W.; Seff, Karl *J. Am. Chem. Soc.* **1977**, *99*, 7057.
(32) Good, M. L. "Mössbauer Effect Data Index"; Stevens, J., Stevens, V., Eds.; IFC/Plenum: New York, 1972; p 51.
(33) Kim, Yang; Seff, Karl *J. Am. Chem. Soc.* **1977**, *99*, 7055.
(34) Jermyn, J. W.; Johnson, T. J.; Vansant, E. F.; Lunsford, J. H. *J. Phys. Chem.* **1973**, *77*, 2964.
(35) Davydov, A. A.; Bell, A. T. *J. Catal.* **1977**, *49*, 332.
(36) Prados, R. A.; Clausen, C. A., III; Good, M. L. *J. Coord. Chem.* **1973**, *2*, 201.
(37) Chao, Chien-Chung; Lunsford, J. H. *J. Am. Chem. Soc.* **1971**, *93*, 71.
(38) Breck, D. W. *J. Chem. Educ.* **1964**, *41*, 678.
(39) Huang, Yun-Yang *J. Am. Chem. Soc.* **1973**, *95*, 6636.
(40) Fenelon, P. J.; Rubalcava, H. E. *J. Chem. Phys.* **1969**, *51*, 961.
(41) Leroi, G. E.; Ewing, G. E.; Pimentel, G. C. *J. Chem. Phys.* **1964**, *40*, 2298.
(42) Davydov, A. A.; Bell, A. T. *J. Catal.* **1977**, *49*, 345.